International Journal of Nanomedicine

Dovepress
open access to scientific and medical research

Open Access Full Text Article

ORIGINAL RESEARCH

Bursting the Virulence Traits of MDR Strain of *Candida albicans* Using Sodium Alginate-based Microspheres Containing Nystatin-loaded MgO/CuO Nanocomposites

This article was published in the following Dove Press journal:
International Journal of Nanomedicine

International Journal of Nanomedicine downloaded from https://www.dovepress.com/
For personal use only.

Sadia Abid[1]
Bushra Uzair[1]
Muhammad Bilal Khan Niazi[2]
Fehmida Fasim[3]
Syeda Asma Bano[4]
Nazia Jamil[5]
Rida Batool[5]
Shamaila Sajjad[6]

[1]Department of Biological Sciences, International Islamic University, Islamabad, Pakistan; [2]School of Chemical & Materials Engineering, National University of Sciences and Technology, Islamabad, Pakistan; [3]Discipline of Biomedical Science, Sydney Medical School, The University of Sydney, Sydney, NSW, Australia; [4]Department of Microbiology, University of Haripur, Haripur, Pakistan; [5]Department of Microbiology & Molecular Genetics, Punjab University, Lahore, Pakistan; [6]Department of Physics, International Islamic University, Islamabad, Pakistan

Introduction: *Candida albicans* is a major opportunistic pathogen that causes a wide range of human infections. Currently available therapeutic agents are limited for treating these fungal infections due to multidrug resistance as well as their nonbiodegradability, poor biocompatibility and toxicity. In order to battle these limitations, we have synthesized a polymeric system as microcarriers to deliver the antifungal drug. The objective of the present study was to immobilize MgO/CuO nanocomposite and nystatin-loaded MgO/CuO nanocomposites in nontoxic, nonimmunogenic, biodegradable and biocompatible sodium alginate microspheres for the first time.

Materials and Methods: Nanoparticle-loaded sodium alginate microspheres were prepared by ionotropic gelation technique using calcium chloride as a cross-linker. Synthesized microspheres were characterized using standard characterization techniques and were evaluated for biological activity against MDR strain of *C. albicans*.

Results: Characterization of microspheres by Fourier-transform infrared spectroscopy confirmed loading of Nys-MgO/CuO NPs, scanning electron microscopy (SEM) revealed rough spherical beads with a highly porous surface having an average size in the range of 8–10 µm. X-ray diffraction (XRD) analyzed its semicrystalline structure. Entrapment efficiency of Nys-MgO/CuO NPs was 80% and release kinetic study revealed sustained and prolonged release of drug in pH 5.5. Flow cytometry analysis showed yeast cell death caused by Nys-MgO/CuO MS exhibits late apoptotic features. In cytotoxicity assay 5–14 mg of microspheres did not cause hemolysis. Microspheres reduced virulence traits of *C. albicans* such as germ tube and biofilm formation were compromised at concentration of 5 mg/mL. Antimicrobial assessment results revealed a pronounced inhibitory effect against *C. albicans*.

Conclusion: The in vitro experiments have shown promising results based on good stability, Nys-MgO/CuO NP-encapsulated microspheres can be used as a prolonged controlled release system against MDR pathogenic *C. albicans*.

Keywords: microspheres, antimicrobial activity, nystatin, *Candida*, metal oxides

Introduction

During recent decades, fungal infections have become a serious health issue contributing substantially to human morbidity and mortality.[1,2] These infections range from superficial to invasive or chronic and the effect of these diseases on human health is not generally appreciated. The pathogenic strains of fungi causing life-threatening fungal diseases include *Cryptococcus* spp., *Fusarium* spp., *Aspergillus*

Correspondence: Bushra Uzair
Department of Biological Sciences, International Islamic University, New Campus, Female Block, Room No. 007, Islamabad, H-10, Pakistan
Tel +92 33 1538 3988
Fax +92 901 9815
Email bushra.uzair@iiu.edu.pk

submit your manuscript | www.dovepress.com
DovePress
http://doi.org/10.2147/IJN.S282305

© 2021 Abid et al. This work is published and licensed by Dove Medical Press Limited. The full terms of this license are available at https://www.dovepress.com/terms.php and incorporate the Creative Commons Attribution – Non Commercial (unported, v3.0) License (http://creativecommons.org/licenses/by-nc/3.0/). By accessing the work you hereby accept the Terms. Non-commercial uses of the work are permitted without any further permission from Dove Medical Press Limited, provided the work is properly attributed. For permission for commercial use of this work, please see paragraphs 4.2 and 5 of our Terms (https://www.dovepress.com/terms.php).

spp., and *Candida* spp. but *Candida albicans* in particular, is the most ubiquitous pathogenic multidrug resistant strain causing invasive fungal infections.[3] To treat these infections, the use of therapeutic agents available presently is limited in terms of their low bioavailability, toxicity, antibiotic resistance and high cost.[4,5] Therefore, there is an increased need to search for new therapeutic options.

Generally, amphotericin B (Amp B) and the azole group of antifungals are the choice of drugs for the treatment of superficial and invasive infections, but excessive use of these drugs has increased the fungal resistance. Nystatin, a polyene macrolide synthesized by *Streptomyces noursei*, is an antifungal agent and has broader spectrum of antifungal activity than antifungal antibiotics like Amp B and azoles.[6] Nystatin exerts its therapeutic effect by forming complexes with ergosterol in plasma membrane leading to intracellular content leakage, but its efficacy is restricted to topical infections because of its significant high toxicity when administered intravenously.[7]

Moreover, many inorganic metal oxides have also attracted the attention as antimicrobial agents due to their improved stability and safety which are lacking in organic metals[8] among the nanoparticles of metal oxides, magnesium oxide NPs have been used to treat various diseases due to their stability under stressful conditions.[9,10] MgO has been used for magnesium supplementation, an important mineral for the human body. MgO shows impressive applications in the medical field such as bone regeneration, heartburn relief and digestive issues, as well as antitumor and antimicrobial agents, and is accepted as a safe biomaterial by the US Food and Drug Administration.[11] Raffi et alreported that copper oxide NPs are very stable, strong and have longer shelf life than organic antimicrobials.[12] Cioffi et al studied the antifungal and bacteriostatic properties of CuO NPs.[13] Studies on antimicrobial activities of both copper oxides and magnesium oxide identified them to be active agents against both fungi and bacteria.[14] But these nanoparticles could be toxic to the human body when administrated directly because of their large and highly reactive surface area.

To overcome the limitations described, special attention has been taken on safe, targeted and modified release, polymer-based delivery systems which provide substantial advantages over the other carrier systems for improved antifungal therapies. Physicochemical properties such as size, surface charge, hydrophilicity, biocompatibility, biodegradability, nontoxicity, high availability and low biopolymer cost have made them a promising alternative.[15,16] Several hydrophilic polymers especially polysaccharides and their derivatives have been used for the synthesis of in-site specific modified release dosage forms.[17] Alginate is an anionic polymer derived from brown seaweed or bacteria, commonly used for decades in several pharmaceutical formulations.[18] It consists of β-D-mannuronic acid (M) and α-L-glucuronic acid (G) repeating units linearly linked by 1.4-glycosidic linkages.[19] Alginate form hydrogels or beads when cross linked with divalent cation such as calcium ion in aqueous solution. This ionotropic gelation is the most universal, simplest and nontoxic method for the synthesis of microspheres and is often employed as supports to deliver bioactive compounds.[20] Based on above considerations, the purpose of the present study was to synthesis nystatin-conjugated MgO/CuO composite encapsulated in sodium alginate microspheres. Furthermore, characteristics of the synthesized microspheres in terms of their size, morphology, crystallinity, chemical structure and bioactive compound loading and release was performed. At last the antifungal activity and effect of developed microspheres on virulence traits of *Candida* was conducted.

Materials and Methods

Materials

Sodium alginate (Gaviscon, Reckitt Benckiser Pakistan Ltd), calcium chloride (Nutriflex Special, B. Braun, Pakistan Pvt), phosphate-buffered saline (PBS, Sigma-Aldrich, USA), fetal bovine serum(FBS, Gibco, Thermo Fisher Scientific, USA), potato dextrose agar (PDA Merck, Germany), sabouraud dextrose agar (SDA, Oxoid Deutschland, Thermo Scientific™, USA), Triton X (Merck, Pvt Ltd, Pakistan), crystal violet (Ricca Chemical, US), nystatin (Wyeth, NJ, USA) were all purchased from commercial vendors. Annexin V binding buffer, propidium iodide and annexin V-FITC kit was obtained from Biolegend. Magnesium oxide and copper oxide nanoparticles were obtained from Nano photocatalysis lab International Islamic University Islamabad.

Preparation of Drug-loaded MgO-CuO Conjugate

Stock solution of 20 µL of nystatin (100,000 units/mL) suspension was prepared by diluting it in 980 µL of sterile water. Further, antibiotic-bound biogenic MgO/CuO

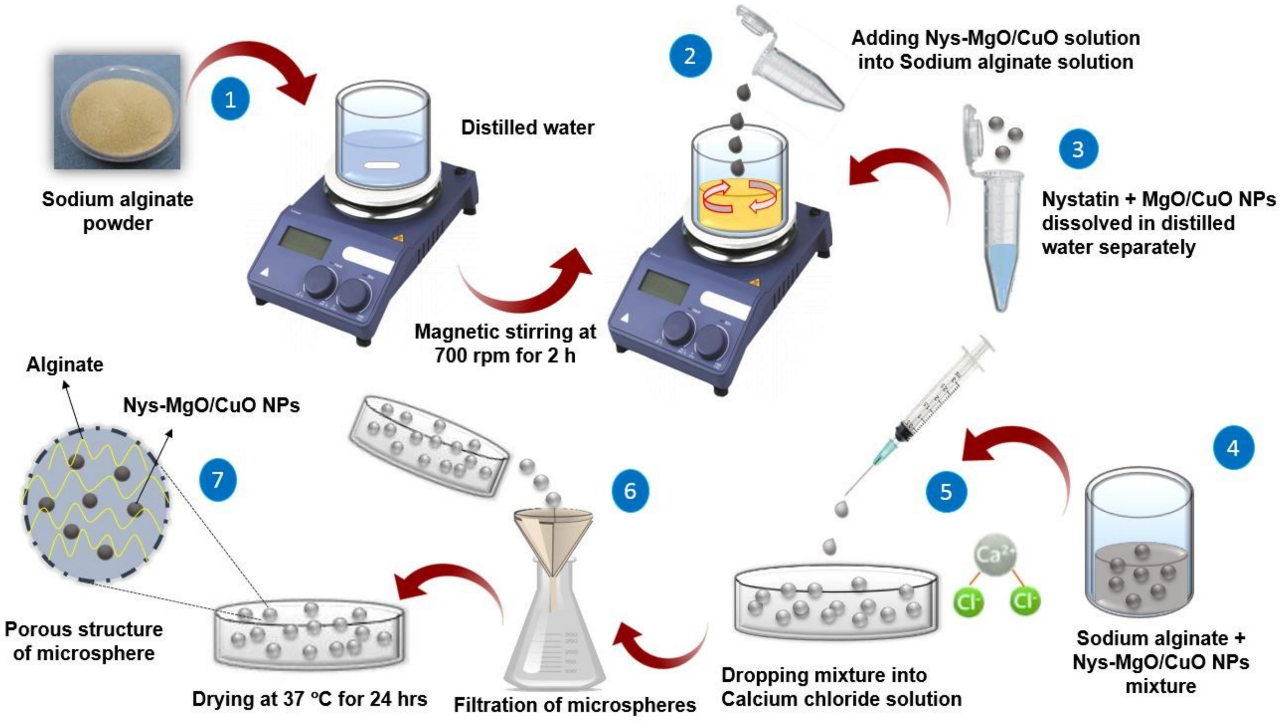

Figure 1 Synthesis of Nys-MgO/CuO nanoparticle-loaded microspheres by ionic gelation method.

nanoparticles were prepared by stirring 1 mL of nystatin solution with 1 mL of biosynthesized MgO/CuO nanoparticles for two hours, followed by incubation for 48 h at room temperature. The subsequent functionalized nanoparticles were centrifuged at 6000 rpm for 10 min, and the pellet was resuspended in sterile deionized water, dried in the drying oven, and stored in dark at 4°C in Eppendorf tubes.

Synthesis of Metal Oxide NP-loaded Microspheres

Synthesis of metal oxide NP-loaded microspheres was performed using same method as Kanokpanont et al.[21] A total of 30 mg of already green synthesized magnesium oxide and copper oxide composite were dissolved in 1 mL of distilled water and stirred separately and 25 mL of sodium alginate solution was prepared by mixing 0.75 g of SA powder in 25 mL of distilled under continuous magnetic stirring for 15 min. Nanoparticles solution was then added to alginate solution and stirred further for two hours. After thorough mixing, the mixture was left for one hour to make it bubble free. This mixture was then passed through a syringe into 50 mL calcium chloride solution. Microspheres formed instantaneously were allowed to harden in the calcium chloride for 15 min and then collected through filtration, washed with distilled water three times and dried for 24 h at room temperature.

Synthesis of Nys-MgO/CuO-loaded Sodium Alginate Microsphere

A 0.75 g of sodium alginate 3% (w/v) was added to 25 mL of distilled water and magnetically stirred for 15 min with gentle heat. Thirty milligrams mg of nystatin-loaded MgO/CuO nanoparticles were added in 1 mL of distilled water in Eppendorf and vortex. This solution was added to sodium alginate solution and stirred up to complete dissolution for two hours. The mixture was allowed to stand for one hour at room temperature to become bubble free. Then 20 mL of sodium alginate solution was pumped slowly into 50 mL of calcium chloride solution (5% w/v) which acted as a cross-linking agent through a syringe with fine stainless-steel needle (0.45 mm in diameter) in a dropwise manner. The distance from the calcium chloride solution to the needle was 6 cm. The microspheres formed immediately and were left for 15 min to harden in the $CaCl_2$ solution. They were then recovered by filtration, washed with distilled water three times and dried at room temperature for 24 h (Figure 1).

Synthesis of Nystatin-loaded Sodium Alginate Beads

Nystatin-loaded microsphere were prepared as a positive control. Briefly, 20 µL of nystatin was dissolved in 2 mL of distilled water and vortex. This solution was added to 0.75 g/25 mL sodium alginate solution and stirred for 30 min. The suspension was elapsed for one hour to remove any air bubbles, introduced into a 5 mL syringe and extruded through a needle into 50 mL of $CaCl_2$ solution. The formed beads were left for 30 min in a solution of $CaCl_2$. Drug-loaded microspheres were collected through filtration, washed thrice with distilled water and dried for 24 h at room temperature. Hollow sodium alginate microspheres were prepared as a negative control applying same method described above.

Nanoparticles Entrapment Efficiency

To determine the concentration of Nys-MgO/CuO conjugate entrapped in microspheres,[22] the microspheres were weighed and dissolve in 25 mL phosphate buffer (pH 6.8). The suspension was sonicated for 15 mins to lyse microspheres and extracted for 12 h. One milliliter of this solution was then dissolved in 10 mL of PBS and absorbance of Nys-MgO/CuO conjugate in phosphate buffer was determined spectometrically at 285.5 nm. Blank microspheres were also assayed as control. Calibration curve regression equation was calculated for the total sum of conjugate. The efficiency of encapsulation was computed using the following formula:

$$\text{Encapsulation Efficiency}(\%) = \frac{\text{Experimental NPs loaded MS (mg)}}{\text{Theoretical NPs loaded MS (mg)}} \times 100$$

Release Kinetic Studies

To evaluate the in vitro release of the nystatin-loaded formulation, a vertical Franz diffusion cell system with dialysis membrane (cutoff mol. weight. 12,000) was used. The cellulose acetate membrane was placed carefully on the upper donor chamber separating the receptor chamber. Acetate buffer (pH 5.5) was added to the receptor chamber to maintain sink condition throughout the studies that facilitate the diffusion rate. Accurately weighed quantity of nystatin-loaded microspheres and Nys-MgO/CuO-loaded MS were placed on the upper chambers and allowed to release in a receptor chamber containing acetate buffer media having pH 5.5 at 30±0.2°C while continuous stirring (100 rpm) for approximately 10 h. Samples (1 mL) were withdrawn from the receptor chamber at 0, 1, 2.4, 8, and 12-h time intervals and restored with equal quantity of fresh buffer. Withdrawn samples were analyzed for drug release by UV method at 305 nm.[23] The absorbance of each sample was noted and percent drug release was determined by the following formula.

$$\%\,\text{drug release} = \frac{\text{ABS of sample (nm)}}{\text{ABS of Standard (nm)}} \times 100$$

Characterization of Microspheres

X-ray Diffraction (XRD) Analysis

Crystalline structure and purity of bead samples were investigated by X-ray diffraction (XRD) in a wide-angle diffractometer, model D8 Advance Bruker equipped with a LynxEye™ at 60 kV and 60 mA current. The samples were irradiated with monochromatic Cu Kα radiations (1.542 Å).2θ was the diffraction angle used with the values ranging from 10 to 90°, respectively.

FTIR Spectroscopy

Fourier-transform infrared (FTIR) spectra (Thermo Nicolet Nexus FTIR) analyzed the functional groups present in the samples. The sample was crushed to fine powder and mixed with potassium bromide KBr. The mixture was compressed to semi-transparent discs by putting a pressure of 10 tons. The spectrum was measured within 4000–400 cm^{-1} range.

FESEM Analysis

To analyze the morphology and particle size of microspheres, scanning electron microscopy (Hitachi SEM SU 3500, Japan) was used with an acceleration voltage of 5 kV and magnification ranging from 25 to 10 k. Randomly selected beads were mounted on the aluminium stub with the help of adhesive double-sided carbon tape, sputter coated with 20 nm gold film and examined in the scanning electron microscope.[24] A few beads were cut with sterile medical blade for cross-sectional examinations.

Strains

Two clinical strains of *Candida albicans* (AH 201) and (AH 267) were used to evaluate the antifungal activity of microspheres. These strains were obtained from the Microbiology Laboratory of Ali Hospital Rawalpindi, Pakistan. The collected strains were incubated for 48 h at 37°C on Sabouraud dextrose agar medium (1% peptone, 1.5% agar, 4% glucose) at pH 5.6. One colony of each

isolate was inoculated in 10 mL of Sabouraud dextrose broth and incubated for 24 h at 37°C. Cells were harvested by centrifugation (1500 rpm) for 10 min and washed with PBS. *Candida* strains were kept as stock cultures in SDA containing 60% glycerol at –80°C for long-term storage.

Antifungal Activity of Synthesized Microspheres

Antifungal susceptibility tests were performed on potato dextrose agar (PDA) plates according to the method of Moeini et alwith slight modifications. Briefly, six to eight beads from two differently synthesized microspheres, MgO/CuO composite loaded microspheres and Nys-MgO /CuO-loaded microspheres were placed on PDA plates swabbed with *C. albicans* from a parent culture and incubated for 24 h at 37°C.[25] Blank SA microspheres were placed as negative control and nystatin-loaded microspheres were placed as positive control. Zone of inhibition was measured the next day.

Effect of Microspheres on Virulence Factors

Germ Tube Development Assay

Germ tube test was performed using the method of Jalal et al with modification to screen the effect of synthesized Nys-MgO/CuO-loaded microspheres on the formation of germ tube.[26] Two to three small colonies of *Candida* were inoculated in a tube containing 0.5 mL of human serum treated with 5 mg of Nys-MgO/CuO-loaded microspheres and incubated for two to three hours at 37°C. After incubation, a drop of culture was transferred to a clean microscope slide to form a smear, a coverslip was placed onto it and examined under a microscope at 40ẋ. Human serum without microspheres was considered as control. For examination of the percentage of germ tubes present, we used light microscope (ECLIPSE TE300, Nikon, Tokyo, Japan); 100 cells were counted each time.

Phenotypic Biofilm Suppression Assay

The effect of Nys-MgO/CuO microspheres on the biofilm production was evaluated by tube method (TM).[27] A loopful of microorganism from overnight culture PDA plate was inoculated into tubes containing 10 mL of Sabouraud dextrose broth supplemented with 1% glucose. The tubes were then incubated for 48 h at 35°C. After incubation, the supernatant was decanted, and tubes were washed with PBS (pH 7) and dried tubes were stained with 0.1% w/v crystal violet for 30 min. Excess stain was eliminated by washing the tubes with distilled water three times. Then tubes were inverted to dry and then detected for biofilm formation. Production of biofilm was deemed positive if a clear film lined the test tube wall. Media containing *Candida* cells without microspheres was considered as control. The inhibition of biofilm formation was analyzed phenotypically by observing color intensity of crystal violet dye and the amount of biofilm formation was scored as 0=absent, 1=weak, 2=moderate, or 3=strong.[28] Experiments were performed in triplicate and repeated three times.

Flow Cytometry Analysis

C. albicans cells were cultured in Sabouraud broth at 37°C until late log phase. The cells were centrifuged to remove supernatant, suspended in PBS supplemented with 2% glucose and counted in a Neubauer chamber. Suspensions containing 10^6 cells/mL were incubated with 10 mg of Nys-MgO/CuO microspheres agent for eight and 24 h. After antifungal treatment, yeast cells were centrifuged, washed and resuspended in PBS. Cells were then incubated with 1% FBS and Annexin V binding buffer for 20 min and then stained with 5 µL propidium iodide and 5 µL Annexin V-FITC. These stained cells were kept in the dark for 30 min at room temperature. Suspension of untreated cells was also stained with PI and Annexin V-FTIC and used as control. After staining, cells were analyzed with FACScan flow cytometer (Beckman Coulter Cytomics FC500).

Efflux of Cytoplasmic Content

Damage to the cell membrane causes cytoplasmic substances such as DNA and RNA to be released from the cell, which can be detected by UV spectrophotometers below 260 nm.[29] Four aliquots of yeast suspensions first containing only Sabouraud broth as negative control, second with 5 mg blank MS as positive control and third and fourth with 5 mg MgO/CuO and Nys-MgO /CuO MS were incubated at 30°C overnight. The mixture was then filtered using 0.22 µm drainage pin filter to remove yeast and microspheres. OD values were monitored under 260 nm UV.

Hemolytic Activity Against Human Erythrocytes

Hemolytic activity of Nys-MgO/CuO MS was evaluated against human erythrocytes. Sterile blood (5 mL) was

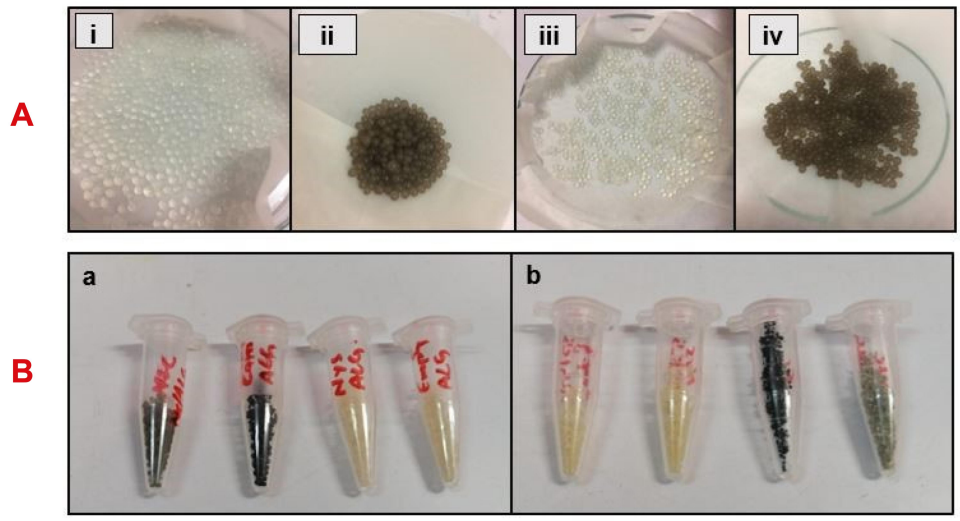

Figure 2 (**A**) Morphology of wet microspheres; sodium alginate beads (i), Mg/CuO composite-loaded SA beads (ii), nystatin loaded SA beads (iii), Nys-MgO/CuO loaded SA beads (iv). (**B**) Morphology of dry microspheres; (a) air dried sodium alginate beads, (b) oven dried sodium alginate beads.

withdrawn from a healthy human after obtaining consent of the participant by briefing her about the study and that the provided blood will be solely used for research purposes. The blood was added directly to 50 mL of sterile blood agar base which was cooled to 45 to 50°C. Flask was swirled immediately to avoid the formation of bubbles and froth on the surface. The mixture was poured immediately into the petri dishes and allowed to solidify. Wells of 6 mm diameter were cut aseptically into the agar and different concentrations of microspheres were added to the wells; two beads (6.6 mg), four beads (13.3 mg), six beads (21 mg) and 0.1% Triton X was used as positive control. Plates were incubated for 24 h at 37°C and then hemolytic reaction (zone of hemolysis around well in millimeters were noted if produced) on plates were observed by holding up the plate to a light source.[30] Formation of a clear visible enlightened area indicate hemolysis of RBCs.

Statistical Analysis

SPSS version 20 (IBM) was used for statistical analysis. Results were expressed as mean ±SD unless otherwise stated. One way ANOVA was applied to the data following Tukey–Kramer test to determine the statistical significance. *P*-value <0.05 was chosen as level of significance.

Results and Discussion

Synthesis of Microspheres

Sodium alginate and drug-composite encapsulated alginate beads were prepared by simple ionic gelation technique by extruding the sodium alginate mixture into aqueous calcium chloride used as cross-linker through a syringe of 24-gauge needle. Morphological images of wet and dry microspheres are presented in Figure 2. Microspheres obtained were spherical and rough in shape. Air dried microspheres were larger in size than oven dried because of inadequate dehydration owing to air drying process.[31,32] Blank sodium alginate microspheres were transparent crystal-like in appearance while nystatin-loaded microspheres were pale yellow. Similarly, microspheres containing only MgO/CuO composite were dark brownish-black while Nys-MgO/CuO-loaded microspheres were light brownish-black in color.

Nanoparticle Entrapment Efficiency

The encapsulation efficacy of Nys-MgO/CuO NPs in sodium alginate was found to be 80%. A possible reason for the high encapsulation efficiency of Nys-MgO/CuO NPs in sodium alginate could be the good solubility of nanoparticles in the solvent, and the close contact between the components.

Release Kinetic Studies

Figure 3 depicts the release profile of nystatin from sodium alginate microspheres and from MgO/CuO SA matrix. Results showed that there is comparatively high release of drug from sodium alginate microspheres encapsulating only drug than from sodium alginate microsphere encapsulating Nys-MgO-CuO NPs. There were two phases in the release profile. The first phase indicates the quick release of the drug, followed by slow release.[33] Our result

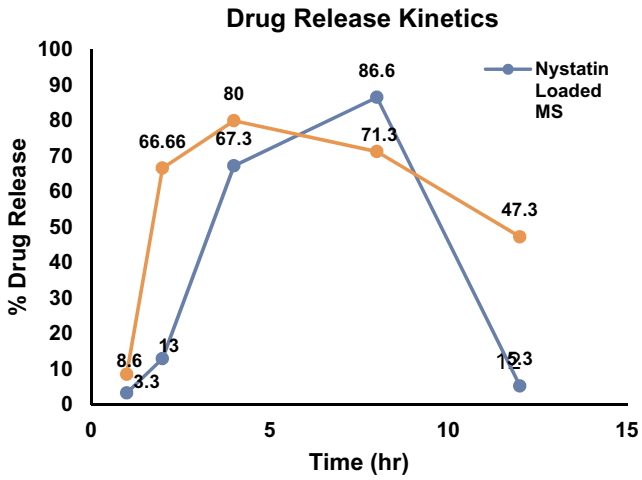

Figure 3 In vitro drug release profile of nystatin from sodium alginate microsphere and from Nys-MgO/CuO-loaded sodium alginate beads.

confirmed that drugs conjugated with MgO/CuO nanoparticles and encapsulated in sodium alginate have increased stability in acid medium and have sustained and prolonged release of drug. This stability and controlled release are attributed by sodium alginate.

Characterization

X-ray Diffraction (XRD)

To investigate the entrapment and physical state of nystatin, MgO/CuO composite and Nys-MgO/CuO conjugate in sodium alginate beads, X-ray diffraction data have been attained. The XRD of blank sodium alginate MS and nystatin-loaded alginate MS are given in Figure 4A. These samples show no distinctive XRD peaks suggesting that the drug was not present in a crystalline state but rather in an amorphous shape in bead matrix.[34] This clearly indicates that a shift in the crystalline state of the drug was caused by ionotropic gelation process during the preparation of beads. Two diffraction peaks at 2θ values 13.5° and 29.8° were observed for sodium alginate due to the reflection of their amorphous (110) plane from glucuronate unit and (200) plane from mannuronate unit. Figure 4B shows XRD pattern for MgO/CuO-loaded alginate MS and Nys-MgO/CuO-loaded alginate MS in semicrystalline structural form. The amorphous structure in Figure 4B ensures the presence of sodium alginate while crystalline structure ensures the presence of MgO/CuO and Nys-MgO/CuO. Diffraction peaks for MgO/CuO nanocomposite observed at 39.6°, 44.2°, 64.7°, 76.2°, and 78.61° represents the crystalline planes at (111), (200), (220), (311), and (222), respectively. An additional peak for CuO was observed at 34.26° representing crystal plane at (−111). The observed diffraction reflections of MgO and CuO are in good agreement with JCPDS card No. 77–2364 and JCPDS card No. 89–2531.[35,36] In XRD patterns of Nys-MgO/CuO-loaded formulation a substantial reduction in peak intensities was noticed. The peak depends on the size of the crystal, but the characteristic nystatin peaks have been integrated with the polymer blend matrix in the present study for Nys-MgO/CuO MS, thus inducing amorphous phase nature. However, in the case of drug-loaded beads, the crystallinity of the drug at the crystal size detection limit is hard to investigate. XRD results suggest nystatin

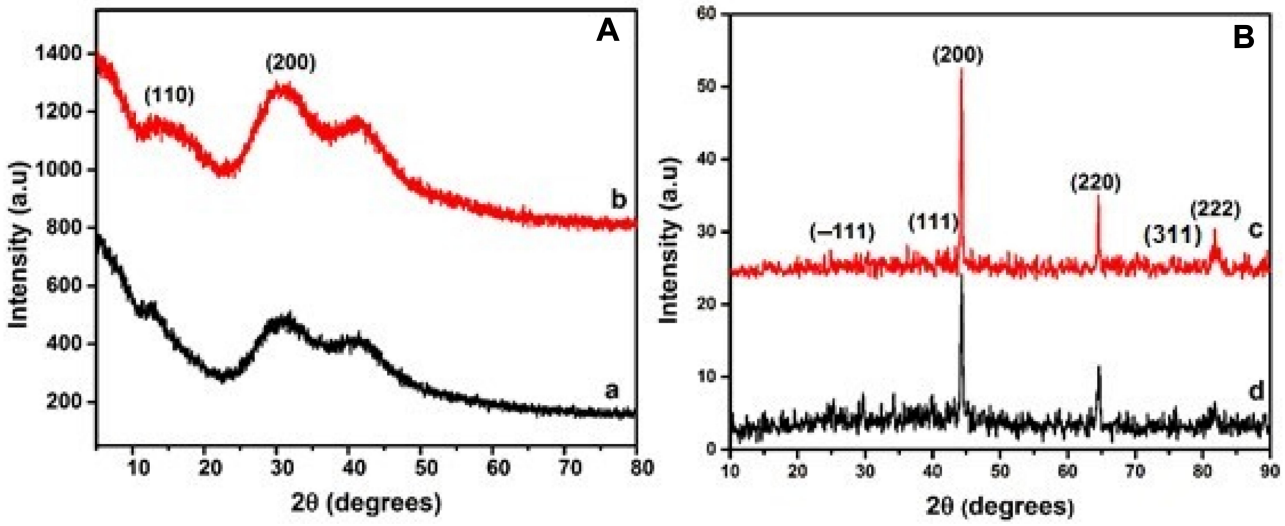

Figure 4 XRD pattern of (**A**) (a) blank sodium alginate MS, (b) Nys-MS, (**B**) (c) MgO/CuO-loaded alginate MS, (d) Nys-MgO/CuO-loaded alginate MS.

dispersion at molecular level in the polymer blend matrix.[37] The crystalline size of MgO/CuO loaded alginate MS and Nys-MgO/CuO-loaded alginate MS samples is measured via Scherrer's equation centered at 44.2° (200) of MgO is found 24.0 and 30.0 nm, respectively.

FTIR Spectroscopy

The FTIR spectrum bands for bare sodium alginate were observed at 3422.5, 2921.8, 1629.5 cm^{-1} (Figure 5a).[38] All samples exhibited broad and wide spectrum at wave number 3600 cm^{-1}–3200 cm^{-1} which is attributed to free hydroxyl group O–H stretching and bending vibrations of water molecules. In the FTIR spectrum of sodium alginate the peak at 1629 cm^{-1} was assigned to $–COO^-$ symmetric stretching. Peak obtained at 2921 cm^{-1} was assigned to $–CH_2$ stretching.[39] The cross-linking of sodium alginate with $CaCl_2$ showed a shift of C=O peak from 1629 cm^{-1} to 1639 cm^{-1} indicating an ionic bonding between calcium ion and carboxyl groups of sodium alginate.[40] The FTIR spectrum of nystatin drug had absorption peaks at wave numbers 3412.2, 2921.7, 1627.3, 1442.2, 1031, 543.1 cm^{-1}. (Figure 5b).[41] The absorption peak at wave number 618 cm^{-1} was assigned to the stretching vibration of Cu-O bonding in monoclinic crystal structure of CuO (Figure 5c and d).[42,43] The characteristic bands at wavenumber 3600–3400, 1639, ~600–800 cm^{-1} were assigned to functional groups of MgO structure.[44] The stretching vibration mode ~600–800 cm^{-1} indicated Mg-O-Mg bonds.[45] Some peaks of nystatin, MgO and CuO overlap somewhat with one another and with the intense peak of sodium alginate. Balamurugan et al investigated the MgO NPs and found the vibration mode in the range of 487–677 cm^{-1} wave number, demonstrating the bonds of Mg-O-Mg.[46]

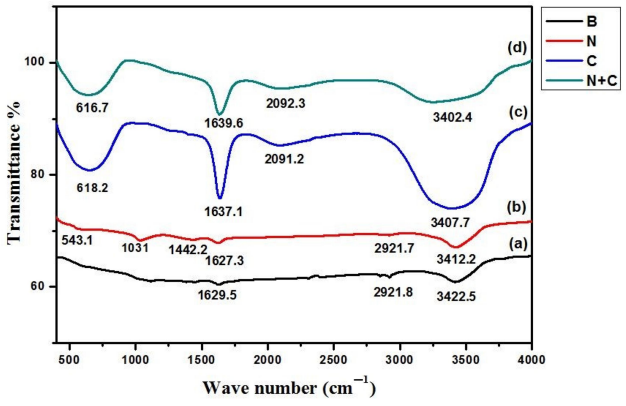

Figure 5 FTIR spectra of (a) sodium alginate MS (b) nystatin-loaded alginate MS, (c) MgO/CuO-loaded alginate MS, (d) Nys-MgO/CuO-loaded alginate MS.

Scanning Electron Microscopy (SEM)

Surface morphology of beads were examined by scanning electron microscopy (SEM). Optical micrographs of beads in Figure 6 illustrate that the beads have a rough spherical shape of average size 8–10 μm and a highly porous surface, which easily allows the diffusion of drug conjugated nanoparticles from microspheres when come into contact with an aqueous environment (Figure 6C, D, G and H). The porous surface observed through SEM also proved the sustained in vitro release of drug from microspheres. It was observed that the size of dried bare sodium alginate microspheres was smaller than other combinations of microsphere and wet bare microspheres were larger in size than other microsphere formulations (Figure 6A). It is evident that nystatin-loaded MS and Nys-MgO/CuO MS (Figure 6B and F), have rougher surface than the other alginate bead formulations. Due to the incorporation of drug and nanoparticles, their surfaces have attained roughness, and increased concentration has made the surface more porous. The morphological features MgO/CuO composite-loaded microspheres shown in Figure 6E suggest rough structures with many cracks ascribed to rapid process of drying.[37] The cross-sectional images of Nys-MgO /CuO-loaded MS (Figure 7) showed that the drug conjugated nanoparticles were found in the inner surface and were dispersed well in the polymer matrix. It also confirmed that the surface of microspheres become permeable upon swelling in aqueous medium.[47]

Antimicrobial Activity

The means of zones of inhibition of *C. albicans* by microspheres at 24 h were measured. Table 1 shows the antifungal activity of synthesized microspheres against *C. albicans*. Nys-MgO/CuO alginate microspheres represented an excellent inhibitory effect against both strains of *C. albicans* than MgO/CuO alginate microspheres in in-vitro. The synergistic activity of Nys-MgO/CuO-loaded sodium alginate microspheres showed zone of inhibition of 24.5±1.7 mm while zone of inhibition of Mg/CuO-loaded sodium alginate microspheres was computed as 19.2±1.6 mm for *C. albicans* strain (AH201). For *C. albicans* strain (AH267) zone of inhibition measured for Nys-MgO/CuO and MgO/CuO microspheres was 14.3 ±1.2 mm and 1.3±0.61 mm respectively. Nystatin-loaded microspheres showed 0.41±0.23 mm and 0.5±0.21 mm.

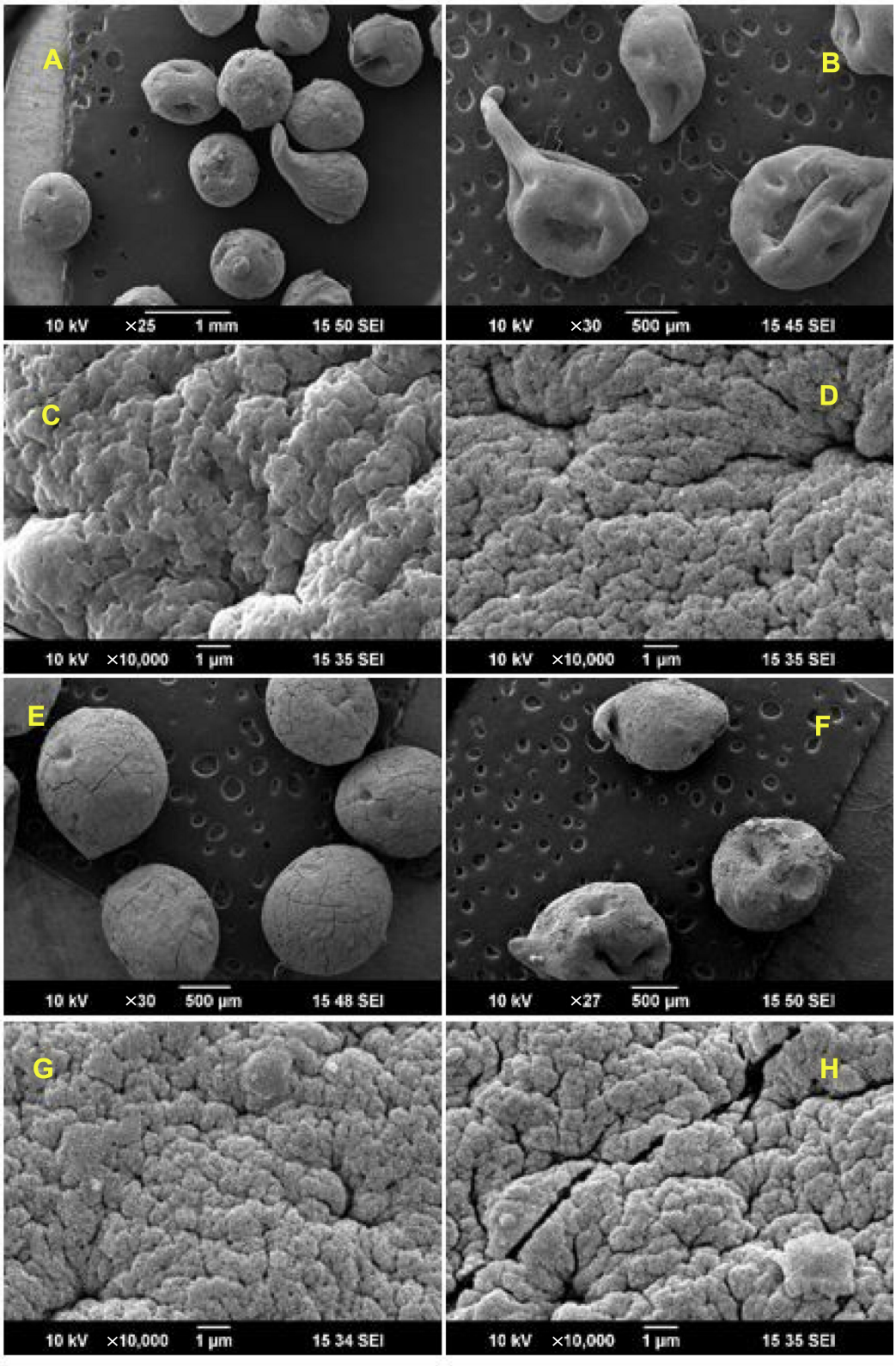

Figure 6 SEM images of blank sodium alginate MS (**A** and **C**), nystatin-loaded alginate MS (**B** and **D**), MgO/CuO-loaded alginate MS (**E** and **G**), Nys-MgO/CuO-loaded alginate MS (**F** and **H**).

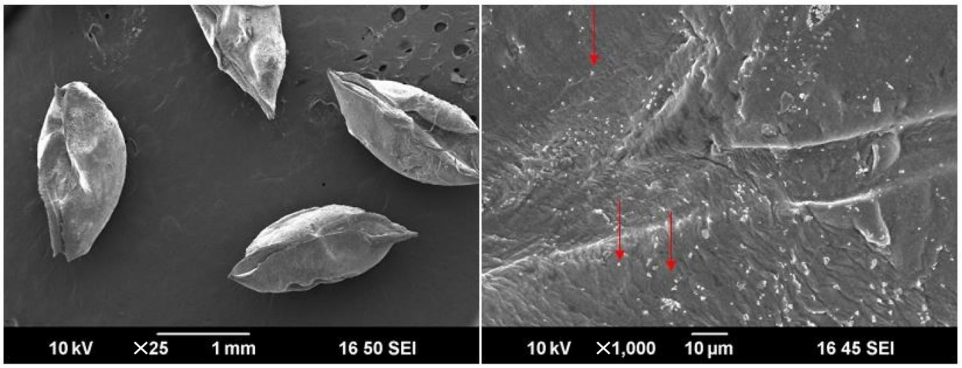

Figure 7 SEM images of cross-section of Nys-MgO/CuO microsphere. Arrows indicates the dispersed nanoparticles.

Sodium alginate microsphere (control) did not demonstrate any antifungal activity in both strains (Figure 8).

CuO NPs in the concentration of 50 µg/mL were used by Khan et al showed higher antimicrobial activity against growth and biofilm formation.[48] A study conducted by Kong et al demonstrated that MgO NPs can efficiently inhibit the growth and two-phase morphological transformation of *C. albicans*.[49] Nystatin antifungal activity on *Candida* was studied previously. For one of them, the bioactivity of 30 µg/mL nystatin was 18–24 mm in agar well diffusion.[50] In another study, nystatin has shown antifungal effect against *C. albicans* at MIC_{50} equal to 25 µg/mL. MIC_{50} standard of nystatin for susceptible *Candida* species is 4–7 µg/mL; therefore, the strains of *Candida* in this study showed considerable resistance to nystatin. However, nystatin has been reported to be successful compared to azole and amphotericin B against resistant strains of *Candida* in clinical trials.[51] Results of our study showed combined antifungal effect of nystatin-loaded MgO/CuO NPs.

Effect on Virulence Factors

Germ Tube Development Assay

The most important virulent factors in *C. albicans* are the morphological transformations between yeast and filamentous forms. Development of germ tube or hyphae initiates adherence and biofilm formation in *C. albicans* which play key role in colonization and hence pathogenesis.Infections could be reduced by blocking the transformation of yeast buds into hyphae. For instance, hyphal-inducing conditions include stimuli such as increased temperature, pH, serum, nutrient hunger, and cell density.[52] In present study, the effect of biosynthesized sodium alginate microsphere encapsulating Nys-MgO/CuO on development of germ tube in clinical isolates of *C. albicans* has been investigated. Germ tube formation is expressed as a percentage of that for control cells incubated in absence of microspheres. Our experiments confirmed that Nys-MgO/CuO-loaded SA microspheres significantly inhibit the serum induced mycelia formation by 75% after 2.5 h of incubation and 92% after three hours of incubation at concentration of 5 mg/mL (Figures 9 and 10).[52,53] Jalal et al published similar findings that silver NPs inhibited germ tube formation at 0.25 mg/mL by 97.1%.[54] In another study, complete inhibition of germ tube formation in *Candida* spp. by CuO NPs at 300 mg/L was reported.[55] However, the exact inhibition mechanism is not clear.

Phenotypic Biofilm Suppression Assay

Biofilm formation is another important virulence trait in *C. albicans*. It plays a key role in pathogenesis.

Table 1 Zone of Inhibition Showed by Synthesized Microspheres Against *Candida albicans*

Microorganism	Zone of Inhibition			
	Sodium Alginate MS (mm) (Control)	Nystatin MS (mm)	MgO/CuO MS (mm)	Nys-MgO/CuO MS (mm)
C. albicans strain (AH 201)	0.0	0.41±0.23*	19.2±1.6***	24.5±1.7***
C. albicans strain (AH267)	0.0	0.5±0.21*	1.3±0.61**	14.3±1.2***

Notes: All values are expressed as mean ±SD. $P<0.05$ compared indicates control group, while *$P<0.05$, **$P<0.01$, and ***$P<0.001$ indicates significance difference from the control group.

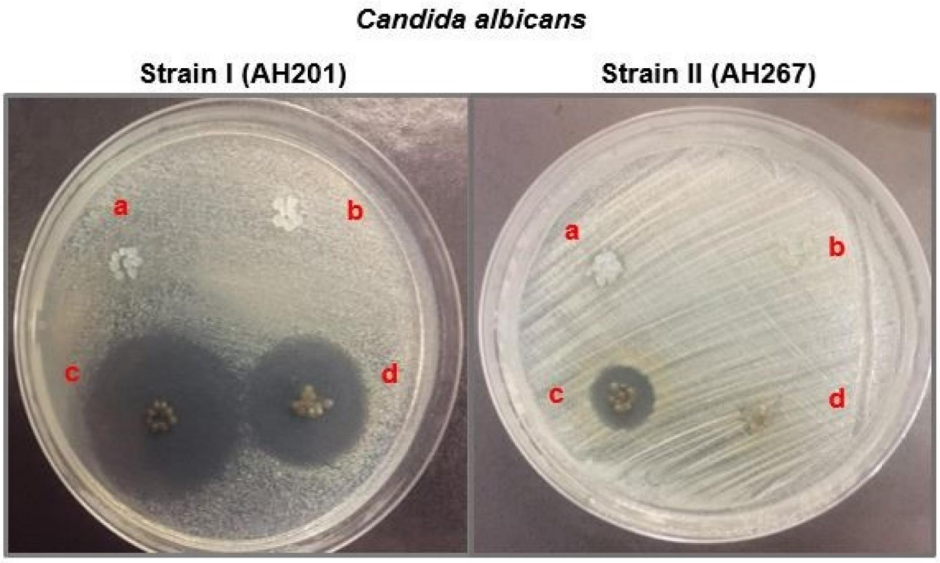

Figure 8 Antimicrobial activity of synthesized microspheres on *Candida albicans* (a) blank SA beads (control), (b) nystatin-loaded SA beads, (c) Nys-MgO/CuO-loaded SA beads, (d) MgO/CuO-loaded SA beads.

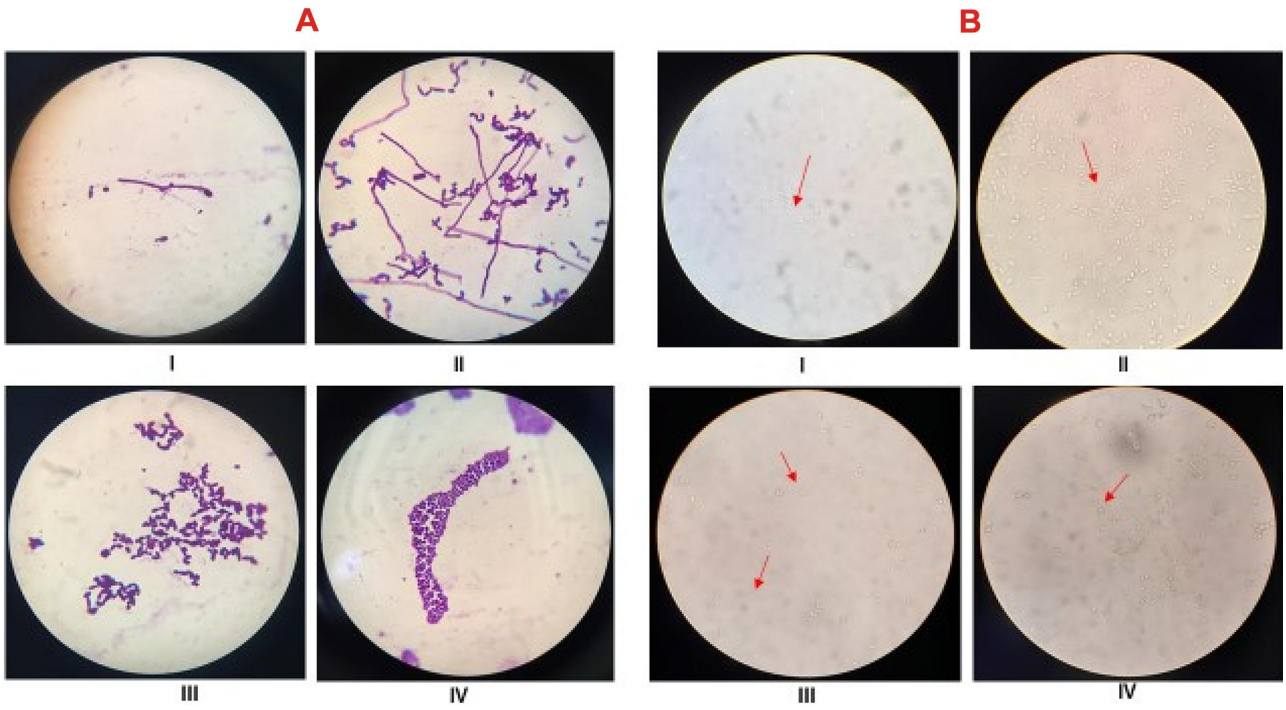

Figure 9 A (stained), **B** (unstained); formation of germ tube in untreated cells after 1 h (I), after 2.5 h (II). Inhibition of germ tube formation in cells treated with Nys-MgO /CuO MS for 2 h (III), for 3 h (IV). The arrows indicate the formation of germ tubes (I, II) and inhibition of growth of germ tubes (III, IV).

C. albicans form a biofilm on medical devices such as urinary catheter, cardiac valves, artificial vascular bypass device and pacemakers. The sessile cells within biofilm act as a barrier for drug diffusion, are highly resistant to drugs, and are difficult to eliminate. Antibiofilm agent for handling such serious infections is therefore urgently required. To some extent, *Candida*'s loss of ability to form biofilm may indicate less virulence when directly invading and colonizing the host tissue (Figure 11). Qualitative suppression of biofilm formation in the presence of Nys-MgO/CuO alginate beads was investigated in the present study by test

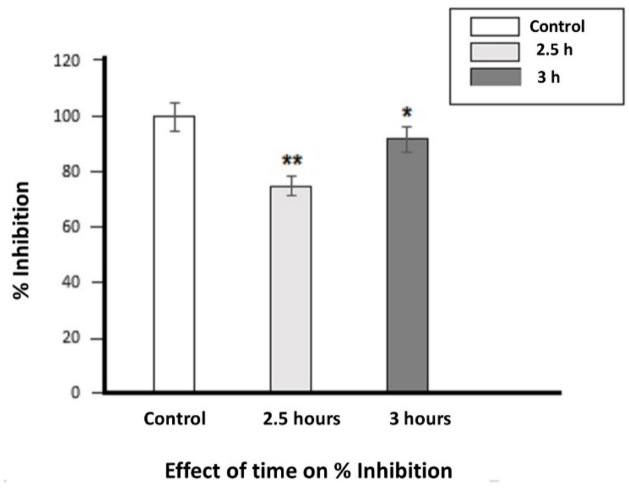

Figure 10 Inhibition of germ tubes in *C. albicans* incubated with Nys-MgO/CuO MS at 2.5 h and 3 h. The data is presented as the mean ±SD and analyzed using ANOVA. *P<0.01 and **P<0.001 refers to statistical significance of both groups from the control.

tube method and biofilm inhibition was examined phenotypically (Figure 12).[56] It was demonstrated that Nys-MgO/CuO alginate microspheres inhibit biofilm formation on tubes when stained with crystal violet (Figure 12B and C) while control untreated normal cells remained bound together within extracellular matrix and formed strong biofilm (Figure 12A). A study by Jalal et al[54] showed complete inhibition of the formation of biofilm in *C. albicans* by Ag NPs. Recently Eshed et al reported that low concentrations of CuO NPs prevent biofilm formation in *Streptococcus mutans*.[57] The antibiofilm effect is primarily due to the interruption of cell wall and enhanced penetration of drug and nanoparticles into the biofilm structure that disturbs cell membrane lipidomes. Inhibition of blastospores and hyphae forms also suppresses the development of biofilms in *C. albicans*.[58]

Flowcytometry

Flow cytometry enables the rapid detection of drug conjugated nanoparticles internalization in live yeast.[59] *C. albicans* exhibited increased damage to cell membrane and leakage of cell inclusion when treated with Nys-MgO /CuO microspheres, as determined by flow cytometry analysis. Phosphatidylserine is a phospholipid enriched in the inner leaflet of the plasma membrane that is exposed to calcium-dependent stimuli in the outer leaflet during early apoptosis.PI, an intact impermeable dye will only move through the cells when they are compromised or dead. In contrast Annexin V-FITC has strong attraction for outer leaflet phosphatidylserine. Consequently, cells can be marked with Annexin V-FITC only for the duration of

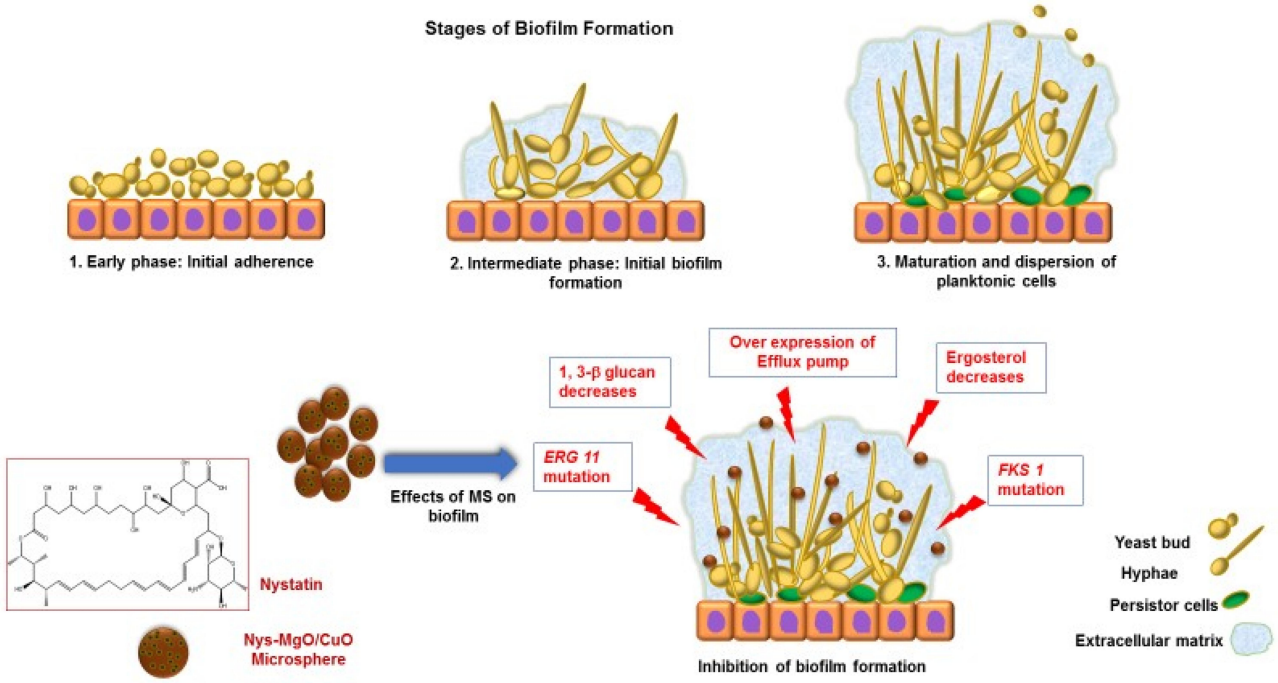

Figure 11 Stages of biofilm formation and effects of Nys-MgO/CuO microspheres on biofilm formation.

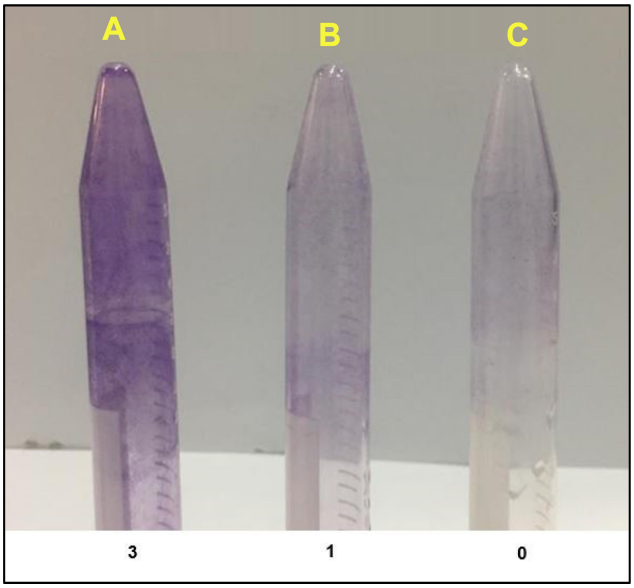

Figure 12 Control untreated cells incubated for 24 h (**A**), cells treated with Nys-MgO/CuO for 24 h (**B**), for 48 h (**C**). Key: score for biofilm formation (0=absent, 1=weak, 2=moderate, 3=strong).

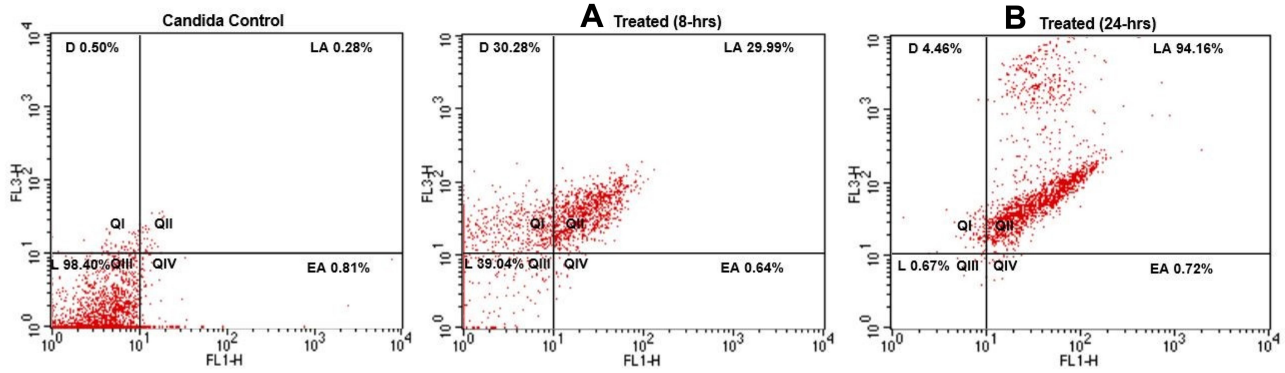

Figure 13 Flow cytometry images of *C. albicans* after incubation with Nys-MgO/CuO for (**A**) 8 h, (**B**) 24 h.

early apoptosis while late apoptotic cells or necrotic cells can be marked with both Annexin V-FITC and PI.[60] In combination with PI, we acquired fast and precise assessment of cellular structural damage based on flow cytometric analysis. Figure 13A revealed 30.28% dead cells (left upper quadrant) and 29.99% late apoptotic cells (right upper quadrant) with incubation time of eight hours and Figure 13B demonstrates 94.16% late apoptotic cells. Our results showed that the cell population in the right upper quadrant in Figure 13B which indicates late apoptotic cells increased to 94.16% with increase in incubation time with Nys-MgO/CuO microspheres (24 h) in comparison to Figure 13A (29.99%) which was incubated for eight hours. We confirmed that the cell death caused by Nys-MgO/CuO MS exhibits late apoptotic features (Table 2). Collectively, the data presents that the Nys-MgO/CuO MS elevated the membrane permeability of the *C. albicans* cells, possibly resulting in cell injury or death.

Table 2 Flowcytometry Results of *C. albicans* Cells Treated with Nys-MgO/CuO

Cell Type	Control	Treated Cells (8h)	Treated Cells (24h)
Live cells	98.40%	39.04%	0.67%
Dead cells	0.50%	30.28%	4.46%
Late apoptotic cells	0.28%	29.99%	94.16%
Early apoptotic cells	0.81%	0.64%	0.72%

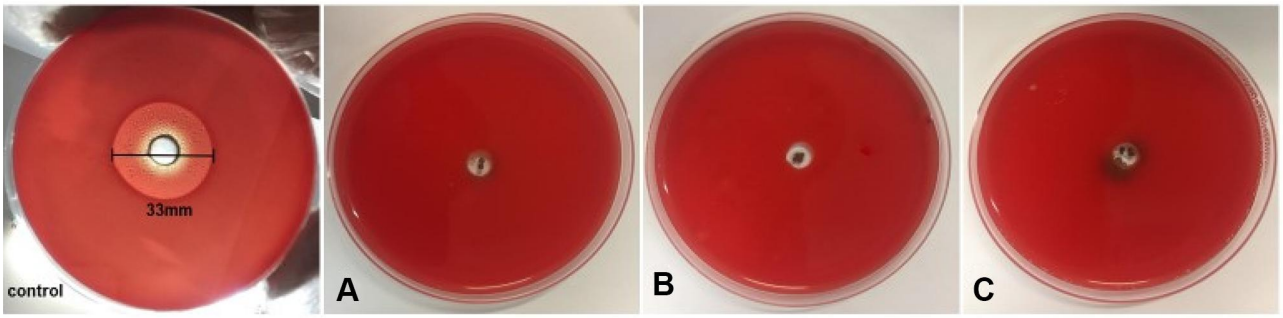

Figure 14 Hemolytic activity of Nys-MgO/CuO MS against human blood at different concentrations key: control showed formation of 33 mm halo due to lysis of RBCs (**A**) 6.6 mg (two beads), (**B**) 14 mg (four beads), (**C**) beads showed hemolysis at conc. of 21 mg (six beads).

Efflux of Cytoplasmic Content

Drug-conjugated antimicrobial nanoparticles exhibit antibiotic activity on the target cell membrane through the formation of pores that cause leaks of important metabolites leading to cell lysis. Disruption of the cell membrane structure is the primary destroying mechanism for antifungal agents. We examined whether Nys-MgO/CuO MS would cause leakage of cellular components. The leakage of cytosolic components was evaluated using cell suspension supernatant preincubated with nystatin loaded MS, MgO/CuO composite loaded MS and Nys-MgO/CuO loaded MS with concentration of (10 mg/10 mL). The absorbance recorded at 260 nm was 0.141 nm, 0.055 nm and 0.096 nm respectively which revealed a significant release of intracellular constituents (DNA or proteins) from severely destroyed membranes of *C. albicans*. This data give evidence for flow cytometry analysis (Figure 13) that the disruption of cell membranes occurred, and cells stained with both annexin V and PI (PI binds with released fragmented DNA).

Hemolytic Activity

Hemolytic activity was assessed by using petri dishes containing nutrient agar supplemented with 5 mL RBCs. However, it allows the evaluation of hemolysis that appears on the agar as an easily visible light region. Results represented in Figure 14A and B showed that Nys-MgO/CuO microspheres exhibited no hemolytic activity, but at a relatively high concentration (Figure 14C). There was absence of enlightenment around the well containing 6 mg and 14 mg Nys-MgO/CuO MS while Triton X (control) showed 33 mm hemolytic halo and a clearly enlightened area. Our result confirmed that at dosage range of 5–14 mg/mL, these microspheres do not exercise any hemolytic effect on human erythrocytes (Table 3). A research carried out by Amiriet al found that CuONPs with a concentration of 100–5000 µg/mL had no toxic impact on human cells.[61] Similarly, a study by Patel et al proved that MgO NPs do not show any significant cytotoxicity at the range 150–250 µg/mL.[62] Boros-Majewska et al also reported that nystatin at low concentrations do not cause cytotoxicity.[63]

Table 3 Hemolytic Activity of Nys-MgO/CuO Microspheres on Human RBCs (Erythrocytes)

Nys-MgO/CuO MS Concentration (mg)	RBC Hemolysis
Control (Triton X)	Clear enlightened area (33 mm halo)
6.6	–
14	–
21	Small enlightened area

Mechanism of Action of Synthesized Microspheres on *Candida albicans*

Nys-MgO/CuO loaded microspheres exhibited positive effects against yeast. Penetration of drug and nanoparticles released from microspheres within fungal cell wall causes denaturation of proteins, inactivation of enzymes, creation of ROS and DNA damage.[64] The release of drug as well as composite might have interacted with the cell membrane permeability by binding with ergosterol, a major component of the cell membrane and forming a polyene-microsphere-ergosterol complex. This complex causes changes in the efflux pump and forms pores in the cell membrane.[65] Leakage of K^+ ion makes the extracellular environment acidic and impairs the metabolism that leads to cell death. Suppression of lanosterol conversion into ergosterol may be caused by inhibition of enzyme 1–4 α demethylase encoded by gene ERG II which

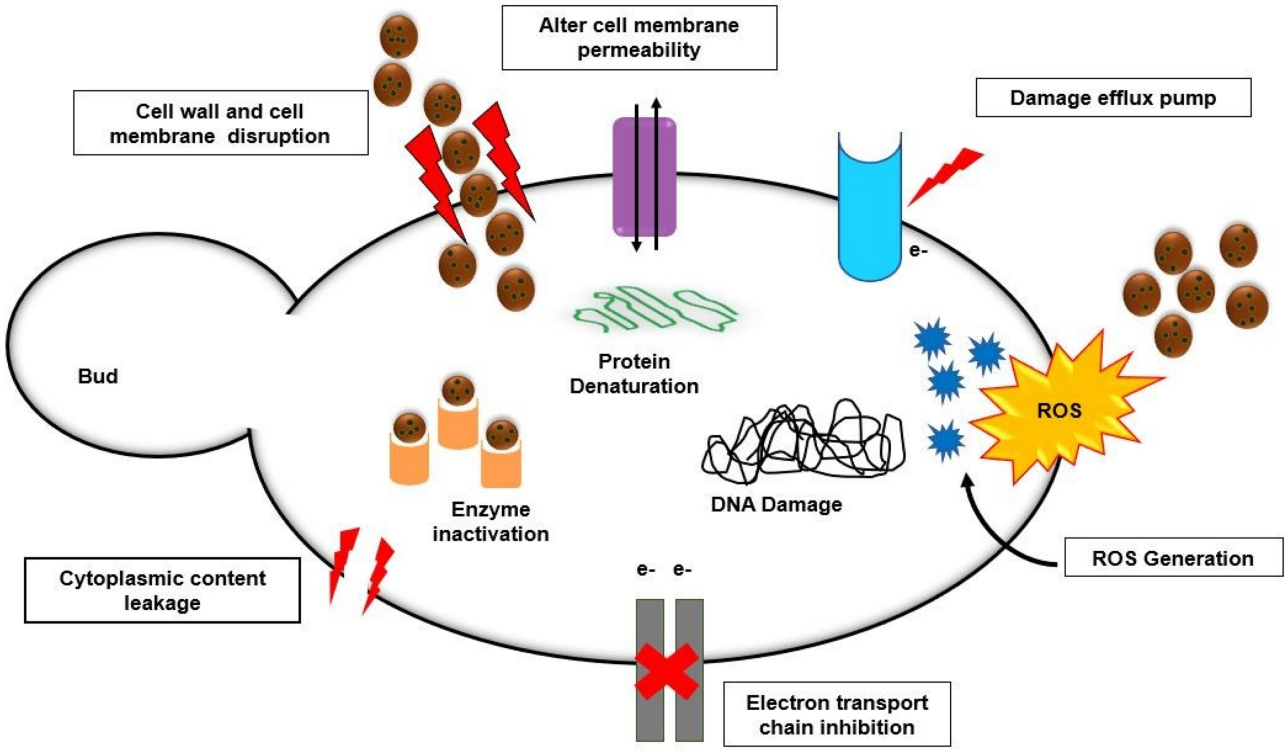

Figure 15 Hypothetical mechanism of action of Nys-MgO/CuO microspheres against *C. albicans*.

is involved in ergosterol biosynthesis. High accumulation of lanosterol causes toxicity and changes in the membrane fluidity and chitin synthase activity. Microspheres may also cause deletion/mutation in gene *FKS1* that will inhibit the activity of 1, 3β glucan synthase leading to disruption in cell glucan synthesis which results in cell wall damage (Figure 11).[66] Moreover, the electrostatic interaction between the cell wall and antifungal material allows the antifungal material to invade the cell and produce ROS which in turns denatures enzymes and proteins and interact with DNA and RNA leading to cytotoxicity and cell apoptosis (Figure 15).[67] Moreover, inhibition of *Candida* morphogenesis by Nys-MgO/CuO nanoparticles invariably inhibit biofilm formation. Cell wall damage and existence of yeast and hyphae forms also inhibit biofilm formation.[68]

Conclusion

This study illustrates the successful development of novel drug-composite loaded microspheres by ionic gelation method for the treatment of *C. albicans* infections. The method of preparation is simple, fast, and inexpensive, and can be performed at room temperature under mild conditions in aqueous surroundings. SEM revealed the size and surface structure of microspheres, and XRD confirmed the purity and crystallinity. FTIR analyzed the functional groups and entrapment of Nys-MgO/CuO nanoparticles. The synergistic activity of drug-conjugated nanoparticles encapsulated in alginate beads exhibited strong anticandidal activity than drug or nanocomposite alone. Flow cytometry revealed cell membrane damage leading to the release of cytoplasmic content and cell death. Toxicity imposed by nanoparticles upon direct contact with the human body was reduced by using a nontoxic, biocompatible, and biodegradable alginate-polymer based antifungal delivery system providing a safe and modified release. The nystatin composite-loaded microsphere systems could be effectively adapted in applications where a sustained release of this antifungal is beneficial to prevent or minimize infections. The obtained microspheres have promising potential in antifungal agent delivery application as anticandidal material. Further, in vivo study must be carried out to explore the biocompatibility and undesired adverse impact of Nys-MgO/CuO MS for their potential therapeutic application.

Ethical Statement

The approval for the use of *C. albicans* strains and human blood sample was taken from the Department of Biological Sciences Ethics and Biosafety Committee of International

Islamic University Islamabad, Pakistan. The blood was provided by a healthy donor with a written informed consent and all experimental procedures carried out in this research work were under careful ethical consideration. The study was conducted in compliance with the Declaration of Helsinki. The blood sample collected was kept strictly confidential at all levels of data processing.

Acknowledgments

The work is acknowledged to International Islamic University, Higher Education Commission of Pakistan (NRPU Grant No. 3660), Institute of Space Science (IST), National Culture Collection of Pakistan (NCCP), Ali Hospital Islamabad, Pakistan and Nano Photocatalysis lab International Islamic University Islamabad.

Disclosure

The authors report no conflicts of interest in this work.

References

1. Alangaden GJ. Nosocomial fungal infections: epidemiology, infection control, and prevention. *Infect Dis Clin*. 2011;25(1):201–225. doi:10.1016/j.idc.2010.11.003
2. Enoch DA, Yang H, Aliyu SH, Micallef C. *The Changing Epidemiology of Invasive Fungal Infections. Human Fungal Pathogen Identification*. Springer; 2017.
3. Pappas PG, Lionakis MS, Arendrup MC, Ostrosky-Zeichner L, Kullberg BJ. Invasive candidiasis. *Nat Rev Dis Primers*. 2018;4(1):1–20. doi:10.1038/nrdp.2018.26
4. Spadari C, Lopes LB, Ishida K. Potential use of alginate-based carriers as antifungal delivery system. *Front Microbiol*. 2017;8:97. doi:10.3389/fmicb.2017.00097
5. World Health Organization. *The Evolving Threat of Antimicrobial Resistance: Options for Action*. Geneva: WHO; 2012.
6. Fernández-Campos F, ClaresNaveros B, Lopez Serrano O, Alonso Merino C, CalpenaCampmany A. Evaluation of novel nystatin nanoemulsion for skin candidosis infections. *Mycoses*. 2013;56(1):70–81. doi:10.1111/j.1439-0507.2012.02202.x
7. Semis R, Nili SS, Munitz A, Zaslavsky Z, Polacheck I, Segal EJ. Pharmacokinetics, tissue distribution and immunomodulatory effect of intralipid formulation of nystatin in mice. *J Antimicrob Chemother*. 2012;67(7):1716–1721. doi:10.1093/jac/dks117
8. Sajjad S, Arshad F, Uzair B, Leghari SAK, Noor S, Maaza M. GO/Ag_2O composite nanostructure as an effective antibacterial agent. *Chem Select*. 2019;4:10365–10371.
9. Ramanujam K, Sundrarajan M, Biology PB. Antibacterial effects of biosynthesized MgO nanoparticles using ethanolic fruit extract of Emblica officinalis. *J Photochem Photobiol B*. 2014;141:296–300. doi:10.1016/j.jphotobiol.2014.09.011
10. Jain A, Wadhawan S, Kumar V, Mehta S. Colorimetric sensing of Fe3+ ions in aqueous solution using magnesium oxide nanoparticles synthesized using green approach. *Chem Phys Lett*. 2018;706:53–61. doi:10.1016/j.cplett.2018.05.069
11. He Y, Ingudam S, Reed S, Gehring A, Strobaugh TP, Irwin P. Study on the mechanism of antibacterial action of magnesium oxide nanoparticles against foodborne pathogens. *J Nanobiotechnology*. 2016;14(1):54. doi:10.1186/s12951-016-0202-0
12. Raffi M, Mehrwan S, Bhatti TM, et al. Investigations into the antibacterial behavior of copper nanoparticles against Escherichia coli. *Ann Microbiol*. 2010;60(1):75–80. doi:10.1007/s13213-010-0015-6
13. Cioffi N, Torsi L, Ditaranto N, et al. Copper nanoparticle/polymer composites with antifungal and bacteriostatic properties. *Chem Mater*. 2005;17(21):5255–5262. doi:10.1021/cm0505244
14. Sawai J, Yoshikawa T. Quantitative evaluation of antifungal activity of metallic oxide powders (MgO, CaO and ZnO) by an indirect conductimetric assay. *J Appl Microbiol*. 2004;96(4):803–809. doi:10.1111/j.1365-2672.2004.02234.x
15. Zafar N, Uzair B, Niazi MBK, et al. Fabrication & characterization of chitosan coated biologically synthesized TiO2 nanoparticles against PDR *E. coli* of veterinary origin. *Adv Polym Technol*. 2020;13. Doi:10.1155/2020/8456024.
16. Voltan AR, Quindos G, Alarcón KPM, Fusco-Almeida AM, Mendes-Giannini MJS, Chorilli M. Fungal diseases: could nanostructured drug delivery systems be a novel paradigm for therapy? *Int J Nanomedicine*. 2016;11:3715. doi:10.2147/IJN.S93105
17. Abedini F, Ebrahimi M, Roozbehani AH, Domb AJ, Hosseinkhani H. Overview on natural hydrophilic polysaccharide polymers in drug delivery. *Polym Adv Technol*. 2018;29(10):2564–2573. doi:10.1002/pat.4375
18. Bajpai S, Saxena SK, Sharma S. Swelling behavior of barium ions-crosslinked bipolymeric sodium alginate–carboxymethyl guar gum blend beads. *React Funct Polym*. 2006;66(6):659–666. doi:10.1016/j.reactfunctpolym.2005.10.019
19. Khong TT, Aarstad OA, Skjåk-Bræk G, Draget KI, Vårum KM. Gelling concept combining chitosan and alginate – proof of principle. *Biomacromolecules*. 2013;14(8):2765–2771. doi:10.1021/bm400610b
20. Pedroso-Santana S, Fleitas-Salazar N. Ionotropic gelation method in the synthesis of nanoparticles/microparticles for biomedical purposes. *Polym Int*. 2020;69(5):443–447. doi:10.1002/pi.5970
21. Kanokpanont S, Yamdech R, Aramwit P. Stability enhancement of mulberry-extracted anthocyanin using alginate/chitosan microencapsulation for food supplement application. *Artif Cells, Nanomed Biotechnol*. 2018;46(4):773–782. doi:10.1080/21691401.2017.1339050
22. Karthika R, Krishnapriya M, Asha P, Sreeja CN. Preparation and evaluation of chitosan sodium alginate carbamazepine microspheres. *Asian J Pharm Clin Res*. 2017;10(3).
23. Mastiholimath V, Gadad A, Iliger S, Iliger SR. Mucoadhesive microspheres of propranolol hydrochloride for nasal delivery. *Indian J Pharm Sci*. 2007;69(3):402–407. doi:10.4103/0250-474X.34550
24. Larosa C, Salerno M, de Lima JS, et al. Characterisation of bare and tannase-loaded calcium alginate beads by microscopic, thermogravimetric, FTIR and XRD analyses. *Int J Biol Macromol*. 2018;115:900–906. doi:10.1016/j.ijbiomac.2018.04.138
25. Moeini A, Cimmino A, Dal Poggetto G, et al. Effect of pH and TPP concentration on chemico-physical properties, release kinetics and antifungal activity of Chitosan-TPP-Ungeremine microbeads. *Carbohydr Polym*. 2018;195:631–641. doi:10.1016/j.carbpol.2018.05.005
26. Jalal M, Ansari MA, Ali SG, Khan HM, Rehman S. Anticandidal activity of bioinspired ZnO NPs: effect on growth, cell morphology and key virulence attributes of Candida species. *Artif Cells, Nanomed Biotechnol*. 2018;46(sup1):912–925. doi:10.1080/21691401.2018.1439837
27. Christensen GD, Simpson WA, Bisno AL, Beachey EH. Adherence of slime-producing strains of Staphylococcus epidermidis to smooth surfaces. *Infect Immun*. 1982;37(1):318–326. doi:10.1128/IAI.37.1.318-326.1982
28. Mathur T, Singhal S, Khan S, Upadhyay D, Fatma T, Rattan A. Detection of biofilm formation among the clinical isolates of staphylococci: an evaluation of three different screening methods. *Indian J Med Microbiol*. 2006;24(1):25. doi:10.4103/0255-0857.19890

29. Chen J, Wang X, Han H. A new function of graphene oxide emerges: inactivating phytopathogenic bacterium Xanthomonas oryzaepv. Oryzae. *J Nanoparticle Res*. 2013;15(5):1658. doi:10.1007/s11051-013-1658-6
30. Accary C, Rima M, Kouzayha A, et al. Open Journal of Hematology. *Medicine*. 2014;1(5):7.
31. Uyen N, Hamid ZA, Nurazreena A. Fabrication and characterization of alginate microspheres. *Mater Today*. 2019;17:792–797.
32. Das MK, Senapati PC. Furosemide-loaded alginate microspheres prepared by ionic cross-linking technique: morphology and release characteristics. *Indian J Pharm Sci*. 2008;70(1):77–84. doi:10.4103/0250-474X.40336
33. Martín-Villena M, Fernández-Campos F, Calpena-Campmany A, Bozal-de Febrer N, Ruiz-Martínez M, Clares-Naveros B. Novel microparticulate systems for the vaginaldelivery of nystatin: development and characterization. *Carbohydr Polym*. 2013;94(1):1–11. doi:10.1016/j.carbpol.2013.01.005
34. Mandal S, Kumar SS, Krishnamoorthy B, Basu SK. Development and evaluation of calcium alginate beads prepared by sequential and simultaneous methods. *Braz J Pharm Sci*. 2010;46(4):785–793. doi:10.1590/S1984-82502010000400021
35. Al-Hazmi F, Alnowaiser F, Al-Ghamdi A, et al. A new large–scale synthesis of magnesium oxide nanowires: structural and antibacterial properties. *Superlattices Microstruct*. 2012;52(2):200–209. doi:10.1016/j.spmi.2012.04.013
36. Shanan ZJ, Hadi SM, Shanshool SK. Structural analysis of chemical and green synthesis of CuO nanoparticles and their effect on biofilm formation. *Baghdad Sci J*. 2018;15(2):211–216. doi:10.21123/bsj.15.2.211-216
37. Angadi SC, Manjeshwar LS, Aminabhavi TM. Novel composite blend microbeads of sodium alginate coated with chitosan for controlled release of amoxicillin. *Int J Biol Macromol*. 2012;51(1–-2):45–55. doi:10.1016/j.ijbiomac.2012.04.018
38. Badita C, Aranghel D, Burducea C, Mereuta P. Characterization of sodium alginate based films. *Rom J Phys*. 2020;65:602.
39. Aprilliza, M. Characterization and properties of sodium alginate from brown algae used as an ecofriendly superabsorbent. In IOP conference series: *materials science and engineering*. 2017;188(1):012019. IOP Publishing. doi:10.1088/1757-899X/188/1/012019
40. Kusuktham B, Prasertgul J, Srinun P. Morphology and property of calcium silicate encapsulated with alginate beads. *Silicon*. 2014;6(3):191–197. doi:10.1007/s12633-013-9173-z
41. Venkateswaran C, Mohamed P, Janakiraman K. Formulation and evaluation of nystatin vaginal tablet. *Der Pharmacia Sinica*. 2017;8(1):1–10.
42. Radhakrishnan AA, Beena BB. Structural and optical absorption analysis of CuO nanoparticles. *Indian J Adv Chem Sci*. 2014;2(2):158–161.
43. Venkataprasanna K, Prakash J, Vignesh S, et al. Fabrication of Chitosan/PVA/GO/CuO patch for potential wound healing application. *Int J Biol Macromol*. 2020;143:744–762. doi:10.1016/j.ijbiomac.2019.10.029
44. Khaleel WA, Sadeq SA, Alani IAM, Ahmed MHM. Magnesium oxide (MgO) thin film as saturable absorber for passively mode locked erbium-doped fiber laser. *Optics Laser Technol*. 2019;115:331–336. doi:10.1016/j.optlastec.2019.02.042
45. Balakrishnan G, Velavan R, Batoo KM, Raslan EH. Microstructure, optical and photocatalytic properties of MgO nanoparticles. *Results Phys*. 2020;16:103013. doi:10.1016/j.rinp.2020.103013
46. Balamurugan S, Ashna L, Parthiban P. Synthesis of nanocrystalline MgO particles by combustion followed by annealing method using hexamine as a fuel. *J Nanotechnol*. 2014;2014:1–6. doi:10.1155/2014/841803
47. Akalin GO, Pulat M. Preparation and characterization of nanoporous sodium carboxymethyl cellulose hydrogel beads. *J Nanomater*. 2018;2018:9676949. doi:10.1155/2018/9676949
48. Khan ST, Ahamed M, Al-Khedhairy A, Musarrat J. Biocidal effect of copper and zinc oxide nanoparticles on human oral microbiome and biofilm formation. *Mater Lett*. 2013;97:67–70. doi:10.1016/j.matlet.2013.01.085
49. Kong F, Wang J, Han R, et al. Antifungal activity of magnesium oxide nanoparticles: effect on the growth and key virulence factors of Candida albicans. *Mycopathologia*. 2020;185(3):485–494. doi:10.1007/s11046-020-00446-9
50. Khoshkholgh-Pahlaviani MRM, Massiha AR, Issazadeh K, Bidarigh S, Giahi M, Ramtin M. Evaluation of antifungal activity of methanol extract of Acacia (Anagalisarvensis) leaves and nystatin against Candida albicans in vitro. *Zahedan J Res Med Sci*. 2013;15(8):39–41.
51. Gunderson SM, Hoffman H, Ernst EJ, Pfaller MA, Klepser ME. In vitro pharmacodynamic characteristics of nystatin including time-kill and postantifungal effect. *Antimicrob Agents Chemother*. 2000;44(10):2887–2890. doi:10.1128/AAC.44.10.2887-2890.2000
52. Rusu E, Radu-Popescu M, Pelinescu D, Vassu T. Treatment with some anti-inflammatory drugs reduces germ tube formation in Candida albicans strains. *Braz J Microbiol*. 2014;45(4):1379–1383. doi:10.1590/S1517-83822014000400031
53. Kim K-J, Sung WS, Moon S-K, Choi J-S, Kim JG, Lee DG. Antifungal effect of silver nanoparticles on dermatophytes. *J Microbiol Biotechnol*. 2008;18(8):1482–1484.
54. Jalal M, Ansari MA, Alzohairy MA, et al. Anticandidal activity of biosynthesized silver nanoparticles: effect on growth, cell morphology, and key virulence attributes of Candida species. *Int J Nanomedicine*. 2019;14:4667. doi:10.2147/IJN.S210449
55. Mudiar R, Kelkar Mane V. Targeting fungal menace through copper nanoparticles and Tamrajal. *J Ayurveda Integr Med*. 2018;11(3):316–321. doi:10.1016/j.jaim.2018.02.134
56. Sharma P, Sambyal S, Shrivastava D, Nadifi S. Phenotypic detection of biofilms in Candida species isolated from various clinical specimen. *Int J Adv Res*. 2017;5:1. doi:10.21474/IJAR01/5166
57. Eshed M, Lellouche J, Matalon S, Gedanken A, Banin E. Sonochemical coatings of ZnO and CuO nanoparticles inhibit Streptococcus mutans biofilm formation on teeth model. *Langmuir*. 2012;28(33):12288–12295. doi:10.1021/la301432a
58. Różalska B, Sadowska B, Budzyńska A, Bernat P, Różalska S. Biogenic nanosilver synthesized in Metarhiziumrobertsii waste mycelium extract–As a modulator of Candida albicans morphogenesis, membrane lipidome and biofilm. *PLoS One*. 2018;13(3):e0194254. doi:10.1371/journal.pone.0194254
59. Ahmad A, Khan A, Kumar P, Bhatt R, Manzoor N. Antifungal activity of Coriarianepalensis essential oil by disrupting ergosterol biosynthesis and membrane integrity against Candida. *Yeast*. 2011;28(8):611–617. doi:10.1002/yea.1890
60. Rieger AM, Nelson KL, Konowalchuk JD, Barreda DR. Modified annexin V/propidium iodide apoptosis assay for accurate assessment of cell death. *JoVE*. 2011;(50):e2597.
61. Amiri M, Etemadifar Z, Daneshkazemi A, Nateghi M. Antimicrobial effect of copper oxide nanoparticles on some oral bacteria and candida species. *J Dent Biomater*. 2017;4(1):347.
62. Patel MK, Zafaryab M, Rizvi M, et al. Antibacterial and cytotoxic effect of magnesium oxide nanoparticles on bacterial and human cells. *J Nanoeng Nanomanufact*. 2013;3(2):162–166. doi:10.1166/jnan.2013.1122
63. Boros-Majewska J, Turczyk Ł, Wei X, Milewski S, Williams DW. A novel in vitro assay for assessing efficacy and toxicity of antifungals using human leukaemic cells infected with C andida albicans. *J Appl Microbiol*. 2015;119(1):177–187. doi:10.1111/jam.12817
64. Muñoz-Escobar A, Reyes-López SY. Antifungal susceptibility of Candida species to copper oxide nanoparticles on polycaprolactone fibers (PCL-CuONPs). *PLoS One*. 2020;15(2):e0228864. doi:10.1371/journal.pone.0228864

65. Mba IE, Nweze EI. The use of nanoparticles as alternative therapeutic agents against Candida infections: an up-to-date overview and future perspectives. *World J Microbiol Biotechnol*. 2020;36(11):1–20. doi:10.1007/s11274-020-02940-0
66. Gutierrez JA, Caballero S, Díaz LA, Guerrero MA, Ruiz J, Ortiz CC. High antifungal activity against candida species of monometallic and bimetallic nanoparticles synthesized in nanoreactors. *ACS Biomater Sci Eng*. 2018;4(2):647–653. doi:10.1021/acsbiomaterials.7b00511
67. Radhakrishnan VS, Dwivedi SP, Siddiqui MH, Prasad T. In vitro studies on oxidative stress-independent, Ag nanoparticles-induced cell toxicity of Candida albicans, an opportunistic pathogen. *Int J Nanomedicine*. 2018;13(T–NANO2014 Abstracts):91. doi:10.2147/IJN.S125010
68. Lara HH, Romero-Urbina DG, Pierce C, Lopez-Ribot JL, Arellano-Jiménez MJ, Jose-Yacaman M. Effect of silver nanoparticles on Candida albicans biofilms: an ultrastructural study. *J Nanobiotechnol*. 2015;13(1):1–12. doi:10.1186/s12951-015-0147-8

International Journal of Nanomedicine Dovepress

Publish your work in this journal

The International Journal of Nanomedicine is an international, peer-reviewed journal focusing on the application of nanotechnology in diagnostics, therapeutics, and drug delivery systems throughout the biomedical field. This journal is indexed on PubMed Central, MedLine, CAS, SciSearch®, Current Contents®/Clinical Medicine, Journal Citation Reports/Science Edition, EMBase, Scopus and the Elsevier Bibliographic databases. The manuscript management system is completely online and includes a very quick and fair peer-review system, which is all easy to use. Visit http://www.dovepress.com/testimonials.php to read real quotes from published authors.

Submit your manuscript here: https://www.dovepress.com/international-journal-of-nanomedicine-journal